

RECENT PROGRESS IN THE STUDIES OF NEUTRON-RICH AND HIGH- Z SYSTEMS WITHIN THE COVARIANT DENSITY FUNCTIONAL THEORY*

A.V. AFANASJEV, S.E. AGBEMAVA, D. RAY

Department of Physics and Astronomy, Mississippi State University
MS 39762, USA

P. RING

Fakultät für Physik, Technische Universität München
85748 Garching, Germany

(Received January 10, 2017)

The analysis of statistical and systematic uncertainties and their propagation to nuclear extremes has been performed. Two extremes of nuclear landscape (neutron-rich nuclei and superheavy nuclei) have been investigated. For the first extreme, we focus on the ground state properties. For the second extreme, we pay a particular attention to theoretical uncertainties in the description of fission barriers of superheavy nuclei and their evolution on going to neutron-rich nuclei.

DOI:10.5506/APhysPolBSupp.10.7

1. Introduction

The physics of neutron-rich (up to the neutron drip-line) and extreme Z superheavy nuclei, and the question of the reliability of theoretical extrapolations to such systems are of paramount importance considering the construction of next generation facilities such as FRIB, FAIR, Superheavy Elements Factory, *etc.* which will be operational in the beginning of next decade. Even with these facilities, the expansion of the experimentally known nuclear landscape will be modest (see Fig. 3 below) and still a huge number of nuclei will be beyond of experimental reach. However, these nuclei are important in nuclear astrophysical processes such as the r-process [1] and fission recycling in neutron star mergers [2].

* Presented at the XXIII Nuclear Physics Workshop “Marie and Pierre Curie”, Kazimierz Dolny, Poland, September 27–October 2, 2016.

Thus, the quality of an extrapolation of model predictions to unknown regions of the periodic chart is an important issue. This quality is characterized by systematic and statistical uncertainties [3]. Statistical uncertainties emerge from the details of the fitting protocol such as the choice of experimental data and the selection of adopted errors; they characterize a given functional. Systematic uncertainties emerge from the underlying theoretical approximations; they characterize a selected group of functionals. In nuclear density functional theories (DFT), there are several major sources of approximations, as for instance the general form of the functional, the range of the effective interaction or the form of its density dependence. In presently used covariant density functional theory (CDFT) [4], the density dependence is introduced either through an explicit dependence of the coupling constants [5–7] or via non-linear meson couplings [8,9]. Point coupling and meson exchange models have an interaction of zero and of finite range, respectively [4,6,7,9]. As a consequence, at present, several major classes of covariant energy density functionals (CEDF) exist dependent on the combination of above mentioned features (see Ref. [10] for detail).

In recent years, a number of comprehensive investigations of systematic uncertainties in the ground state observables and their propagation with particle numbers have been performed by us using the NL3* [9], DD-ME2 [6], DD-ME δ [11], DD-PC1 [7] and PC-PK1 [12] CEDFs as state-of-the-art representatives of above mentioned major classes of CEDFs. These studies cover the properties and related systematic uncertainties of different physical observables for all even–even nuclei with $Z \leq 106$ [10,13], for the position of the two-neutron drip-line [10,13,14], for octupole deformed [15] and superheavy nuclei [16]. Note that the analysis of theoretical uncertainties has also been performed in Skyrme DFTs in Refs. [17–20], but the focus was mostly on the statistical uncertainties. In this manuscript, we deal with covariant energy density functionals. In Sect. 2, we investigate the statistical uncertainties in the description of the ground state properties of spherical nuclei and their relation to systematic ones. Section 3 presents a study of statistical and systematic uncertainties in the description of inner fission barriers in superheavy nuclei. Finally, Sect. 4 summarizes our conclusions.

2. Ground state properties of neutron-rich nuclei

Systematic theoretical uncertainties in the prediction of binding energies for the four CEDFs NL3*, DD-ME2, DD-PC1 and DD-ME δ are shown in Fig. 1. While the spreads in the predictions of binding energies stay within 5–6 MeV in the region of the known nuclei [10,14] (see also the region enveloped by solid black line in Fig. 3), they increase drastically when approaching the neutron drip-line where they can reach 15 MeV. This is a consequence of the poorly defined isovector properties of the existing CEDFs.

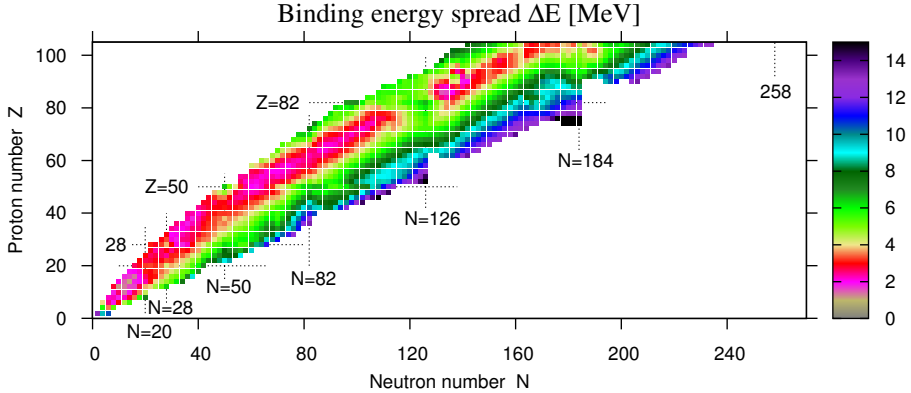


Fig. 1. The binding energy spread $\Delta E(Z, N)$ as a function of proton and neutron number. $\Delta E(Z, N) = |E_{\max}(Z, N) - E_{\min}(Z, N)|$, where $E_{\max}(Z, N)$ and $E_{\min}(Z, N)$ are the largest and the smallest binding energies for each (N, Z) -nucleus obtained with the four covariant energy density functionals NL3*, DD-PC1, DD-ME2 and DD-ME δ . From Ref. [10].

Statistical theoretical uncertainties in binding energies and neutron skins are shown in Fig. 2. These uncertainties are expressed as standard deviations $\sigma(E)$ and $\sigma(r_{\text{skin}})$ for a set of “reasonable” variations of the original functional defined according to Ref. [3]. They are calculated in the spherical relativistic Hartree–Bogoliubov (RHB) framework with the CEDF NL3* for the Ca, Ni, Sn and Pb isotope chains from the two-proton to the two-neutron drip-line. The $\sigma(E)$ values are close to the adopted errors of the fitting protocol for the nuclei used in the fitting. However, they rapidly increase with increasing the neutron number so that for the nuclei in the vicinity of the two-neutron drip-line, they reach values comparable with the spreads in binding energies shown in Fig. 1. This fact should not be used as an argument in favor of the similarity of statistical and systematic uncertainties for binding energies since the inclusion of the results obtained with the CEDF PC-PK1 (limited so far to the isotopic chain with $Z = 70$) shows that systematic uncertainties increase by a factor of around 2.5 as compared with those presented in Fig. 1. Note that the addition of the PC-PK1 results is not expected to alter much the spreads of binding energies within the limit of nuclei reachable with FRIB [14].

It is interesting to compare our results of the analysis of statistical uncertainties with Skyrme results based on the functional UNEDF0 [18, 19]. While the statistical uncertainties are similar for binding energies in both approaches (compare Fig. 1 in Ref. [19] with Fig. 2(a) in the present paper), they are substantially smaller for the neutron skins in relativistic results (compare Fig. 2 in Ref. [18] with Fig. 2(b) in the present paper).

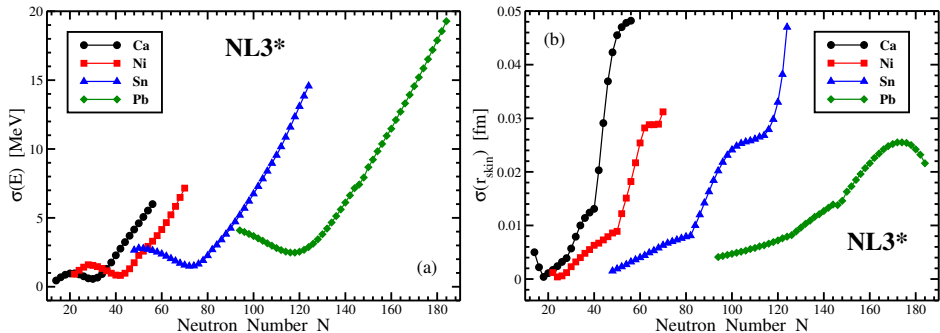


Fig. 2. Statistical uncertainties in binding energies (panel (a)) and neutron skins (panel (b)). All even–even nuclei between the two-proton and two-neutron drip-lines are included.

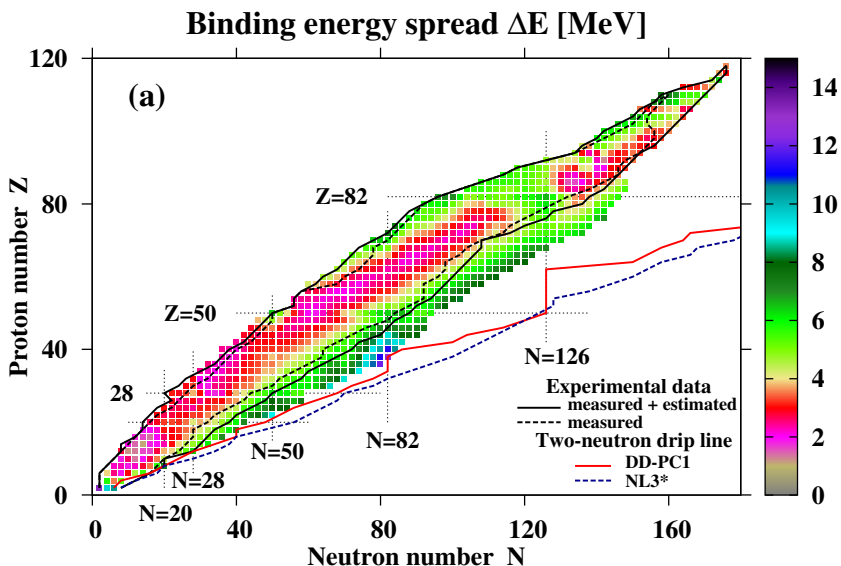


Fig. 3. (Color online) The impact of future measurements on the nuclear landscape. The squares show the results presented in Fig. 1 but only for the nuclei which are currently known and which will be measured with FRIB. The regions of the nuclei with measured and measured+estimated masses are enclosed by dashed and solid black lines, respectively. The squares beyond these regions indicate the nuclei which may be measured with FRIB. The line formed by the most neutron-rich nucleus in each isotope chain accessible with FRIB is called as “FRIB limit”. The same colormap as in Fig. 1 is used here, but the ranges of particle numbers for the vertical and horizontal axis are different from the ones in Fig. 1. The two-neutron drip-lines are shown for the CEDFs NL3* and DD-PC1 by dashed/blue and solid/red lines, respectively. From Ref. [14].

The increase of statistical and systematic uncertainties on approaching the neutron drip-line clearly poses a challenge for theory. In CDFT, it is dominated by the isovector channel of the effective interaction and its density dependence. For example, the freezing of the coupling constant for the ρ -meson in the functional NL3* during a selection of “reasonable” functionals leads to statistical uncertainties at the neutron drip-line which are substantially smaller than those seen in Fig. 2. However, an improvement of the isovector channel is not that simple. Two possible ways have been considered in Ref. [14]. First, new mass measurements with future rare isotope beam facilities will, in principle, improve isovector properties of the CEDFs in the $Z \leq 50$ nuclei (where, according to Fig. 3, most of the data will be measured). However, the improvement is expected to be modest. Second, the improvement in nuclear matter properties will not substantially reduce the uncertainties in the description of neutron-rich systems.

3. Fission barriers in superheavy nuclei

Another extreme of the nuclear landscape (high- Z extreme) is the region of superheavy elements (SHE). The structure of SHEs has recently been reexamined within CDFT in Ref. [16]. This led to significant revisions in our understanding of their structure. Contrary to the previous CDFT studies, it was found that the impact of the $N = 172$ spherical shell gap on the structure of SHEs is very limited. Similar to non-relativistic functionals, some covariant functionals predict an important role played by the spherical $N = 184$ gap. For these functionals (NL3*, DD-ME2, and PC-PK1), there is a band of spherical nuclei along and near the $Z = 120$ and $N = 184$ lines. However, for other functionals (DD-PC1 and DD-ME δ) oblate shapes dominate at and in the vicinity of these lines. The available experimental data on SHEs are, in general, described with comparable accuracy with these functionals. This makes it impossible to discriminate between their predictions for nuclei outside the presently known region.

The stability of SHEs is defined by the fission barriers. Thus, the study of systematic and statistical uncertainties in the predictions of fission barriers has been undertaken using the same set of CEDFs as in Sect. 2.

Statistical uncertainties in the deformation energy curves and fission barriers are illustrated in Fig. 4 on the example of the nucleus ^{296}Cn . The calculations are performed within the axial RHB framework with the functional NL3* [9]. Statistical uncertainties are quantified by the standard deviations in energy σ_E around the mean value of energy. These quantities are defined as a function of deformation for a set of “physically reasonable” functionals using the formalism of Refs. [3, 21]. They are small in the vicinity of the spherical minimum but then they grow with increasing deformation. They become especially pronounced in the vicinity of the inner and outer saddles

and in the region of the superdeformed (SD) minimum. Statistical uncertainties decrease substantially and stabilize above the outer fission barrier. The calculations with the functional DD-ME2 lead to comparable results but with a different deformation dependence of statistical uncertainties [22]. Both calculations suggest that the increase of statistical uncertainties at some deformation may be due to the underlying single-particle structure. This is because the variations of the functional lead to modifications of the single-particle energies as well as to changes in the sizes of the superdeformed shell gaps and the single-particle level densities at the saddles and the SD minimum. These changes then affect the shell correction energies.

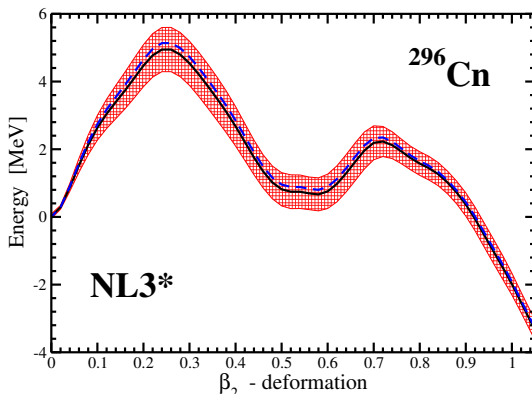


Fig. 4. (Color online) Statistical uncertainties in the deformation energy curves of the nucleus ^{296}Cn . The mean potential energy curve is shown by a solid black line. The gray dashed/red region shows the standard deviations in energy. The potential energy curve obtained with the original functional NL3* is shown by a dashed/blue line.

The systematic uncertainties obtained in axially symmetric RHB calculations for inner fission barrier heights are summarized in Fig. 5. The consideration here is restricted to three CEDFs, namely, NL3*, DD-PC1 and PC-PK1. These functionals, fitted only to the ground state properties of very limited set of nuclei (see details in Ref. [10]) successfully describe experimental fission barriers in the actinides [23–27]. Theoretical uncertainties, expressed in terms of the ΔE^B spreads, are typically less than 2 MeV for the $N \leq 180$ nuclei; only in few nuclei around $Z = 110, N \sim 164$ and $Z \sim 110, N \sim 176$ these uncertainties are higher reaching 4 and 5.5 MeV respectively. However, these uncertainties increase by roughly 1 MeV for the nuclei with $N \geq 182$. It is also important to mention that theoretical spreads in the inner fission barrier heights do not form a smooth function of proton and neutron numbers; there is always a random component in their behavior.

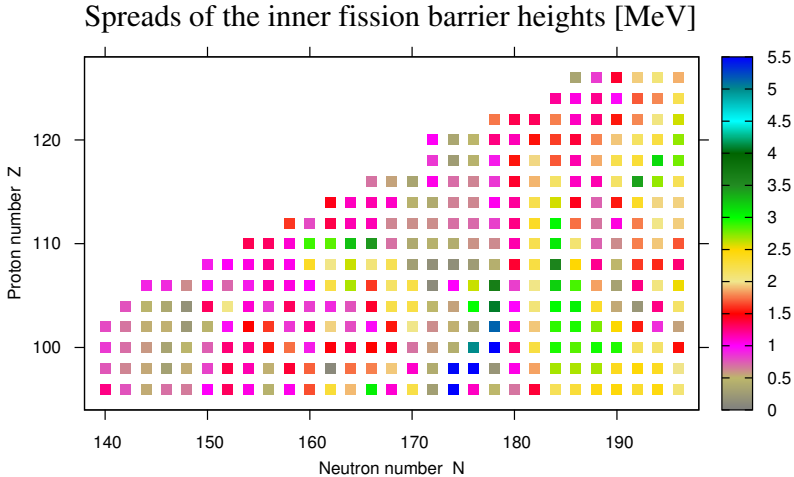


Fig. 5. The spreads ΔE^B of the heights of the inner fission barriers as a function of proton and neutron number. $\Delta E^B(Z, N) = |E_{\max}^B(Z, N) - E_{\min}^B(Z, N)|$, where, for given Z and N values, $E_{\max}^B(Z, N)$ and $E_{\min}^B(Z, N)$ are the largest and smallest heights of inner fission barriers obtained in axial RHB calculations with the set of functionals NL3*, DD-PC1, and PC-PK1.

It is well-known that inner fission barriers in many SHEs are affected by triaxiality; its impact is especially pronounced in the nuclei near the $Z = 120$ and $N = 184$ lines (Ref. [24]). This is exemplified in Fig. 6 for the nucleus $^{302}_{120}$ by potential energy surfaces (PESs). In this nucleus, the triaxial saddles (labeled ‘Tr-Ax’, ‘Tr-A’, ‘Tr-B’) are located at $(\beta_2 \sim 0.32, \gamma \sim 22^\circ)$, $(\beta_2 \sim 0.43, \gamma \sim 34^\circ)$, and $(\beta_2 \sim 0.50, \gamma \sim 22^\circ)$ for the functionals DD-ME2, PCPK1, NL3* and DD-PC1. The ‘Tr-A’ and ‘Tr-B’ saddles are also present in the PES for DD-ME δ , but for this functional, the ‘Tr-Ax’ saddle is shifted to smaller β_2 and γ deformations. The axial saddle is higher in energy than the lowest in energy triaxial saddle for all functionals. Note that the topology of the PES for the functional DD-ME δ differs substantially from the one for other functionals.

The accounting of triaxiality in the calculations modifies the spreads in the predictions of the heights of inner fission barriers. This is clearly seen in Fig. 7 where these spreads, obtained in axial and triaxial RHB calculations, are compared. Although, locally, two calculations may differ slightly, on average, there are strong correlations in the spreads obtained in the two calculations. This suggests that also for other regions of the nuclear chart, not covered by the present triaxial RHB calculations, the spreads in inner fission barrier heights obtained in the axial RHB calculations (see Fig. 5) could be used as a reasonable estimate of the spreads which would be obtained in the calculations with triaxiality included.

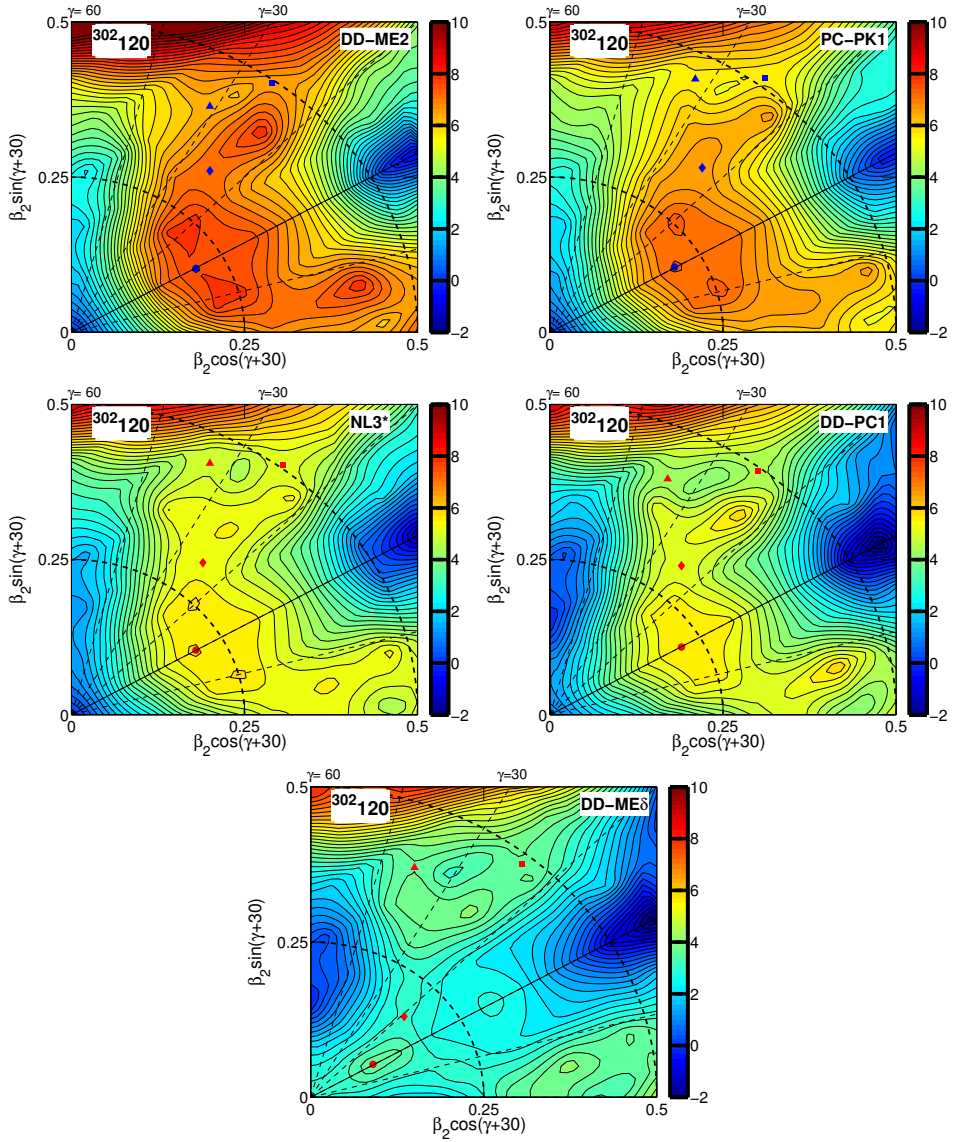


Fig. 6. (Color online) Potential energy surfaces of the nucleus $^{302}_{120}$ as obtained in the calculations with the indicated CEDFs. The energy difference between two neighboring equipotential lines is equal to 0.25 MeV. The Ax, Tr-Ax, Tr-A and Tr-B saddles are shown by blue/red circles, diamonds, triangles, and squares, respectively. The PES are shown in the order of decreasing height of the inner fission barrier.

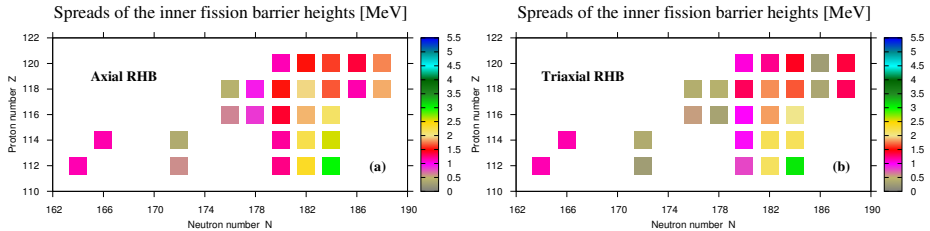


Fig. 7. The same as in Fig. 5 but for a selected set of the $Z = 112$ – 120 nuclei. Panels (a) and (b) show the spreads ΔE^B obtained in axial and triaxial RHB calculations, respectively.

The benchmarking of the functionals to experimentally known fission barriers in the actinides reduces the number of suitable functionals to three (NL3*, DD-PC1 and PC-PK1). This allows to decrease theoretical uncertainties in inner fission barrier heights since the ΔE^B spreads for five functionals are substantially higher than those presented in Figs. 5 and 7 (see also the discussion in Ref. [22]). This fact is also clearly seen in Fig. 6. Even those reduced uncertainties of the inner fission barrier heights translate into the uncertainties of many orders of magnitude for spontaneous fission half-lives (see Ref. [22]).

4. Conclusions

In order to quantify theoretical predictions for covariant density functional theory in unknown regions of the nuclear chart, systematic uncertainties deduced from the results of a set of different well-known covariant energy density functionals, as well as statistical uncertainties derived according to Ref. [3] for a set of “reasonable” variations of one functional, are discussed for ground state observables such as binding energies and neutron skin thicknesses over entire nuclear chart and for inner fission barriers in superheavy nuclei. It is found that the statistical uncertainties are usually smaller than the systematic ones. We observe a systematic growth of the uncertainties for increasing deviations from the experimentally known regions, in particular, when approaching the neutron drip-line or the region of superheavy nuclei with extreme Z values.

Of course, the present investigations are restricted to the mean field level. Employed covariant energy density functionals are fitted to nuclear matter properties and to ground state properties of finite nuclei, such as binding energies and charge radii. Therefore, one can expect that in the future, when we are able to take into account the beyond mean field effects in a microscopic way not only at the model level but also in the fitting protocols, the predictive power of CDFT will considerably increase with appropriate reduction in systematic and statistical uncertainties.

This material is based upon work supported by the Department of Energy National Nuclear Security Administration under Award Number DE-NA0002925, by the U.S. Department of Energy, Office of Science, Office of Nuclear Physics under Award Number DE-SC0013037, and by the DFG cluster of excellence “Origin and Structure of the Universe” (www.universe-cluster.de).

REFERENCES

- [1] M.R. Mumpower, R. Surman, G.C. McLaughlin, A. Aprahamian, *Prog. Part. Nucl. Phys.* **86**, 86 (2016).
- [2] S. Goriely, A. Bauswein, H.-T. Janka, *Astrophys. J* **738**, L32 (2011).
- [3] J. Dobaczewski, W. Nazarewicz, P.-G. Reinhard, *J. Phys. G* **41**, 074001 (2014).
- [4] D. Vretenar, A.V. Afanasjev, G.A. Lalazissis, P. Ring, *Phys. Rep.* **409**, 101 (2005).
- [5] S. Typel, H.H. Wolter, *Nucl. Phys. A* **656**, 331 (1999).
- [6] G.A. Lalazissis, T. Nikšić, D. Vretenar, P. Ring, *Phys. Rev. C* **71**, 024312 (2005).
- [7] T. Nikšić, D. Vretenar, P. Ring, *Phys. Rev. C* **78**, 034318 (2008).
- [8] J. Boguta, R. Bodmer, *Nucl. Phys. A* **292**, 413 (1977).
- [9] G.A. Lalazissis *et al.*, *Phys. Lett. B* **671**, 36 (2009).
- [10] S.E. Agbemava, A.V. Afanasjev, D. Ray, P. Ring, *Phys. Rev. C* **89**, 054320 (2014).
- [11] X. Roca-Maza *et al.*, *Phys. Rev. C* **84**, 054309 (2011).
- [12] P.W. Zhao, Z.P. Li, J.M. Yao, J. Meng, *Phys. Rev. C* **82**, 054319 (2010).
- [13] A.V. Afanasjev, S.E. Agbemava, D. Ray, P. Ring, *Phys. Lett. B* **726**, 680 (2013).
- [14] A.V. Afanasjev, S.E. Agbemava, *Phys. Rev. C* **93**, 054310 (2016).
- [15] S.E. Agbemava, A.V. Afanasjev, P. Ring, *Phys. Rev. C* **93**, 044304 (2016).
- [16] S.E. Agbemava, A.V. Afanasjev, T. Nakatsukasa, P. Ring, *Phys. Rev. C* **92**, 054310 (2015).
- [17] J. Erler *et al.*, *Nature* **486**, 509 (2012).
- [18] M. Kortelainen *et al.*, *Phys. Rev. C* **88**, 031305 (2013).
- [19] Y. Gao *et al.*, *Phys. Rev. C* **87**, 034324 (2013).
- [20] J.D. McDonnell *et al.*, *Phys. Rev. Lett.* **114**, 122501 (2015).
- [21] S. Brandt, *Data Analysis. Statistical, Computational Methods for Scientists, Engineers*, Springer International Publishing, Switzerland, 2014.
- [22] S.E. Agbemava, A.V. Afanasjev, D. Ray, P. Ring, submitted to *Phys. Rev. C*.
- [23] H. Abusara, A.V. Afanasjev, P. Ring, *Phys. Rev. C* **82**, 044303 (2010).
- [24] H. Abusara, A.V. Afanasjev, P. Ring, *Phys. Rev. C* **85**, 024314 (2012).
- [25] B.-N. Lu, E.-G. Zhao, S.-G. Zhou, *Phys. Rev. C* **85**, 011301 (2012).
- [26] V. Prassa, T. Nikšić, G.A. Lalazissis, D. Vretenar, *Phys. Rev. C* **86**, 024317 (2012).
- [27] B.-N. Lu, J. Zhao, E.-G. Zhao, S.-G. Zhou, *Phys. Rev. C* **89**, 014323 (2014).